Chemistry—Methods

Research Article
doi.org/10.1002/cmtd.202500052

Chemistry Europe
European Chemical Societies Publishing

www.chemistrymethods.org

Quantitative X-Ray Fluorescence Imaging to Evaluate the Efficacy of Micro-Structured Cellulose Foams and Poultices in Wall Painting Desalination

Martina Romani,* Olivia Gómez-Laserna,* Francesco Caruso, Jaime García Garrido, Alvaro Tejado, Anna Nualart-Torroja, África Pitarch Martí, Erlantz Lizundia, and Maite Maguregui*

The crystallization of soluble salts poses a significant challenge to mural painting conservation. While cellulose poultices are widely used to desalinate mural paintings due to their high absorption and ease of handling, their effectiveness within the porous network of wall paintings remains a complex issue. For the first time, this study explores the potential of micro-structured cellulose-based foams as an alternative to conventional poultices for desalinating fresco wall paintings. A laboratory experiment compared the efficacy of foams and poultices, using fresco wall painting mock-ups (produced with the Roman technique) that were vacuum-impregnated with salt solutions (chlorides, sulfates, and mixtures). Short and long application times were considered, and foam reusability across multiple application cycles was assessed. Micro-energy dispersive X-ray fluorescence (μ-EDXRF) imaging was employed to quantitatively evaluate salt content reduction, both superficially and throughout the mock-up stratigraphy. Results show that foams are considerably more effective than poultices, achieving a salt removal efficiency between 6 and 10 times higher. The uniform micro-porous foam network enables faster desalination, reducing treatment risks and minimizing waste while supporting circular economy principles. This study also demonstrates the utility of μ-EDXRF imaging in monitoring desalination efficacy for both surface and cross-section analyses when assessing new desalination protocols.

1. Introduction

Salt crystallization is one of the most significant conservation problems affecting wall paintings, as it can lead to severe degradation of these heritage objects over time.[1–4] Salt crystallization damage is primarily due to the crystallization pressure exerted by salts as they form and grow within the material's pores. This pressure results from repulsive disjoining forces between salt crystals and the mineral surfaces of the pore walls. These forces prevent direct contact between the growing salt crystals and the pore walls, maintaining a thin liquid film that allows the crystals to continue growing and exerting stress on the surrounding material.[5–7] Crystallized soluble salts can undergo cycles of dissolution and recrystallization due to environmental

M. Romani, O. Gómez-Laserna
Department of Analytical Chemistry
Faculty of Science and Technology
University of the Basque Country UPV/EHU
Barrio Sarriena s/n, 48940 Leioa, Spain
E-mail: martina.romanir@ehu.eus
olivia.gomez@ehu.eus

F. Caruso,[+] M. Maguregui
Department of Analytical Chemistry
Faculty of Pharmacy
University of the Basque Country UPV/EHU
Paseo de la Universidad 7, 01006 Vitoria-Gasteiz, Spain
E-mail: maite.maguregui@ehu.eus

J. García Garrido, A. Tejado
TECNALIA
Basque Research and Technology Alliance (BRTA)
Area Anardi 5, 20730 Azpeitia, Spain

A. Nualart-Torroja, Á. Pitarch Martí
Research Group Conservació-Restauració del Patrimoni (AGAUR, 2021 SGR 00089)
Department of Arts and Conservation Restoration
Faculty of Fine Arts
University of Barcelona (UB)
Pau Gargallo 4, 08028 Barcelona, Spain

Á. Pitarch Martí
Institut d'Arqueologia de la Universitat de Barcelona (IAUB)
c/ Montalegre 6-8, 08001 Barcelona, Spain

E. Lizundia
Life Cycle Thinking Group
Department of Graphic Design and Engineering Projects
Faculty of Engineering in Bilbao
University of the Basque Country (UPV/EHU)
Torres Quevedo Ingeniariaren Plaza 1, 48013 Bilbao, Spain

E. Lizundia
BCMaterials
Basque Center for Materials, Applications and Nanostructures, UPV/EHU
Science Park, Bldg. Martina Casiano, 48940 Leioa, Spain

[+]Present address: Conservation Center, Institute of Fine Arts (IFA), New York University (NYU), 14 E 78th Street, 10075 New York, NY, USA

Supporting information for this article is available on the WWW under https://doi.org/10.1002/cmtd.202500052

physico-chemical processes, promoting the formation of cracks, fissures or even flaking, scaling and pigment loss.[8] Besides, some soluble salts have also a role in other degradation phenomena like discoloration of pigments. Examples of this last are chlorides, which may take part in the discoloration of the precious cinnabar pigment, widely used in Roman times to decorate wall paintings.[9,10]

Prior to implementing any desalination protocol in wall paintings, it is necessary to evaluate the composition of crystallized salts and the extent of its diffusion in the wall.[11] This assessment should also determine whether the salt content exceeds a threshold that may potentially lead to damage in the artwork. Given that mural paintings can be situated outdoors, environmental control is seldom feasible. Moreover, in most cases, identifying and blocking the sources of soluble salts in mural paintings is highly challenging, often leading to the necessity of eventual desalination actions.[12] Once the need for desalination has been established, the process of salt removal involves inherent risks such as uncontrolled water release, salt redistribution and creation of salt gradients.[13] Therefore, although water acts as a vehicle that facilitates the removal of salts, its presence should be controlled in desalination interventions to avoid the mentioned conservation problems.

To remove efflorescences from mural paintings, mechanical methods are usually applied using scalpels or brushes.[11] Apart from the physical removal, to facilitate the extraction of salts from the porous structure of wall painting, the most common method involves the application of poultices composed of absorbent materials. Traditionally, the main used for this purpose has been cellulose fibers of different length (typically, between 200 and 700 μm).[14] These can be used without additives or mixed with clay minerals, such as sepiolite or kaolin.[14,15] Their application process involves an initial wetting phase within the poultice-wall system. During this phase, water is transferred from the wet poultice to the dried wall, initiating the dissolution of salts. Subsequently, during salt extraction, the dissolved salt ions migrate back to the poultice as saline solutions. This transport is governed by diffusion and advection forces through concentration gradient driven by the Brownian motion and/or by capillary water flux.[11,16] Materials with a pore size distribution smaller than that of the substrate increase wicking rates, facilitating a higher extraction capacity during the drying and wetting phases. Furthermore, high water retention properties contribute positively to the extraction process until the concentration equilibrium is reached within the system[17] in the wall painting. However, depending on the porous network, the used poultice may not always be fully effective in the mobilization of salts deep in the painting stratigraphy.[18]

Specifically for sulfate removal from mural paintings, Ferroni method or barium hydroxide method has been widely employed since 1970s.[19–21] This desalination protocol consisted in the application of ammonium carbonate and barium hydroxide in aqueous solution or by poultice to extract soluble sulfates from wall painting and form $Ca(OH)_2$ in the mural's pores. In this way, an additional consolidation of the wall painting through natural carbonatation is promoted. However, barium hydroxide is toxic and highly alkaline, potentially affecting sensitive pigments of the wall painted surface. To reduce these risks, the use of nanotechnologies has increased, specifically for wall painting consolidation.[19]

As the most widely available biobased polymer on Earth, cellulose, and fibrillated cellulose offer the functional requisites for highly absorbent materials while adhering to circularity and sustainability principles.[22–24] Microscale cellulose-based systems such as foams or sponges[25] have shown a high efficacy in the adsorption of pollutants from water.[25–28] However, they have not been explored yet in the field of conservation to desalinate wall paintings. In particular, cellulosic foams resulting with microstructured uniform porous networks offer higher water uptake, large active surface area, and enhanced water flux behavior, properties of high interest for salt removal purposes.[29,30] However, implementing this material in heritage conservation practices needs specifically designed testing methodologies that thoroughly examine the capacities of both new and traditional materials based on cellulose.

In recent years, additional materials, such as gels (e.g., agar, poly (vinyl alcohol), or poly (2-hydroxy-ethyl methacrylate)/poly (vinylpyrrolidone)) have been investigated for salt removal on water-sensitive porous materials.[31,32] These pilot studies have demonstrated their potential to remove salts, thus making them interesting alternate materials for desalination of wall paintings. However, the depth of desalination with these gels has not been investigated, nor has it been confirmed whether possible salt redistribution phenomena occur during the desalination process.

An indirect and noninvasive alternative to evaluate the efficacy of salt removal consists in monitoring the ionic conductivity of the absorbent materials before and after being applied on the surface of the artwork.[33,34] If samples (or a salt solution) can be extracted from the wall, ion chromatography can be used to evaluate quantitatively the desalination capacity.[35] This destructive, slow, and expensive approach provides quantitative information on salt removal, but nothing says about the spatial distribution of salts after desalination. In some studies, mortar samples have been extracted from desalinated walls at different depths, solubilizing the remaining salts and quantifying them by ion chromatography.[13,36] This approach can help to better understand the extent of desalination.

An alternative to evaluate the desalination efficacy across the thickness of the specimen could be the use of chemical imaging techniques. Some authors have used micro-energy dispersive X-ray fluorescence (μ-EDXRF) to evaluate the removal of metallic stains from stone surfaces and to monitor the cleaning of photographs;[37,38] however, no references about the use of μ-EDXRF imaging for validating the efficacy of desalination protocols exist.

This study presents, for the first time, a noninvasive methodology based on quantitative μ-EDXRF imaging to evaluate the effectiveness of micro-structured cellulosic foams in the desalination of wall paintings. Ultimately, we aim to demonstrate that these foams are a reusable and more efficient alternative to traditional cellulose poultices used in the field. A series of laboratory-scale experiments was carried out using fresco painting mock-ups impregnated with chlorides, sulfates and a mixture of both. To assess desalination performance, different application times (ranging from minutes to several hours) were tested for each cellulose-based material. Quantitative elemental distribution maps,

Research Article
doi.org/10.1002/cmtd.202500052
Chemistry Europe
European Chemical Societies Publishing

representative of each salt, were generated from the μ-EDXRF hyperspectral data cubes using the fundamental parameters (FP) approach. A comparative study of quantitative distribution maps of elements associated with soluble salts is presented to evaluate, at the microscopic scale, the spatial reduction of salt content on the surface of the mock-ups and within the paintingstratigraphy.

2. Results and Discussion

2.1. Salt Removal Capacity of Cellulose Poultices Versus Foams

Based on traditional desalination practices,[39–42] short (5, 15, 30, and 60 min) and extended application times (8 and 24 h) were applied for both poultices and foams. Each cellulosic material was applied onto four mock-ups, previously infiltrated with chlorides and sulfates.

To evaluate the reduction of salt concentration in the mock-ups by using the poultices and foams, the sum EDXRF spectrum associated to the scan of the whole mock-ups acquired before and after each desalination procedure has been used. Mock-ups were scanned both superficially and in cross section to compare if the desalination procedure is equally effective superficially and through the stratigraphy of the painting.

By scanning superficially, for a short application of 5 min a 98 ± 1% of chlorine reduction was observed using foams (**Figure 1**a). Longer application times (equal or above 1 h) did not offer significant improvements. Therefore, by superficial analysis of the mock-ups, it seems that the desalination is completely effective in a few min.

Upon superficial examination, poultices demonstrated the efficacy of removing 84.3 ± 0.3% of the chloride content within 5-minute application. On the contrary, the poultices required 1 h to remove the same percentage of chlorides as foams removed during a 5-minute application. This result demonstrated that foams exhibit a superior ability to remove superficially chlorides compared to poultices. This effect may be attributed to their enhanced water retention capacity and the larger surface area in direct contact with the surface of the painting.[27]

The whole stratigraphy of the mock-ups was also scanned by μ-EDXRF before and after desalination experiments. In this case, also with foams almost a complete reduction of chlorides (92.5 ± 0.6%) was obtained after 5 min of application. The extraction percentages remained stable for 8 and 24 h of application, with fluctuations of less than 3.0 ± 0.5%. Consequently, back diffusion phenomena were probably compensated by the activation of the dryness phase into foam-painting system.[11,16] The average concentration data of both, surface and profile, seems to be in accordance and pointed out that chloride salt could rapidly

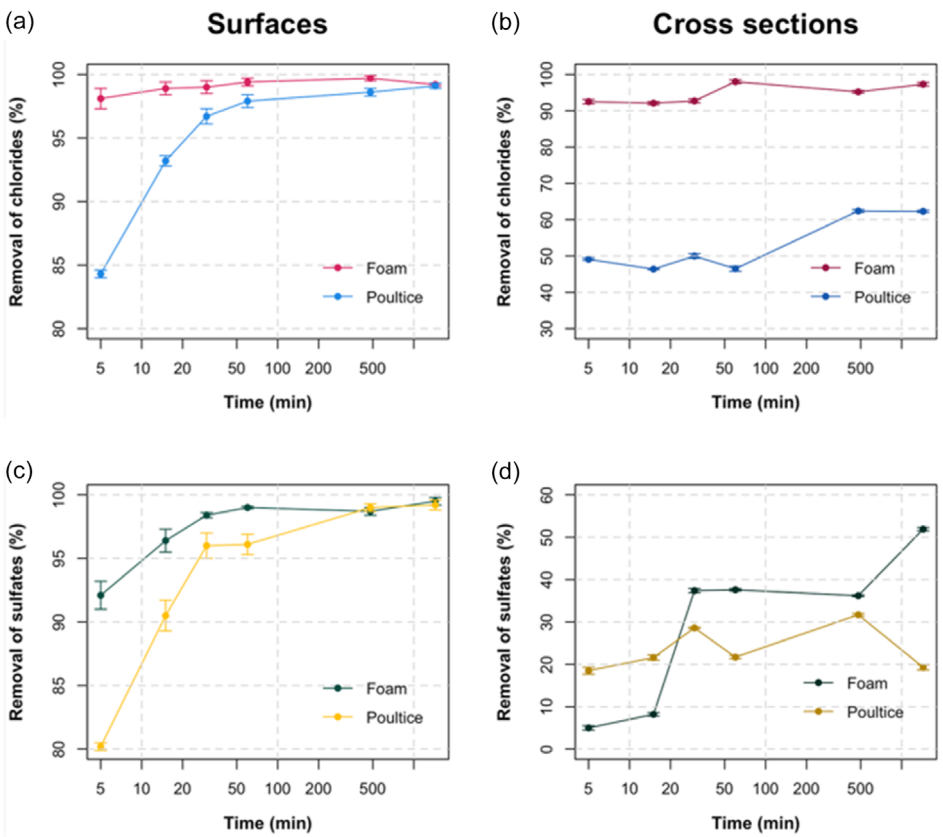

Figure 1. Percentage removal of chlorides a,b) and sulfates c,d) from surfaces a,c) and cross sections b,d) of the studied mock-ups for our micro-structured foam and for the tested poultice. *y*-axes of percentage removal have been cropped to highlight differences in the efficiency of the compared systems. *x*-axes have logarithmic representations to better appreciate trends at low and high times.

mobilize through the porous mock-up network and overpass the interface between the *arriccio* and *intonaco*.

In contrast, a single application of poultices for 5 min led to an incomplete desalination. A $49.1 \pm 0.3\%$ of removal was achieved from the first 5 min to 1 h, exhibiting fluctuations of approximately $4.0 \pm 0.6\%$, until reaching the maximum removal of $62.4 \pm 0.4\%$ after 8 h. Despite the high mobility of chlorides, this result suggests the accumulation of new chloride crystallizations in intermediate zones of the stratigraphy. This phenomenon suggests that the poultice-painting system was primarily governed by the advection process, which accelerates the mobilization of chlorides toward the surface during poultice drying. In this context, the pore size and active area of the cellulose-based material are crucial in enhancing wicking rates from the painting to the poultice.[43]

Both types of cellulose-based materials exhibited lower extraction capacity for sulfates (Figure 1b). Specifically, foams were able to extract $92 \pm 1\%$ of sulfates within 5 min. This value increases up to $99.0 \pm 0.2\%$ at 1 h. On the contrary, the poultices can remove $80.2 \pm 0.3\%$ according to the superficial measurements within 5 min of application. However, their extraction capacity increases to the highest levels between 8 and 24 h (evaporation-driven transport).

The information extracted from the cross section was different compared with the surface analysis. Data extracted from the section showed that foams can reduce $5.0 \pm 0.5\%$ of sulfates within the first 5 min, increasing the value up to $37.4 \pm 0.5\%$ with an additional application of 25 min. Extending the application up to 8 h, no clear changes were observed. Only an increase in the sulfate removal up to $51.9 \pm 0.4\%$ was registered after a cycle of 24 h. The problems observed to extract sulfates from inner areas are associated to the lower mobility of this salt in comparison with chlorides (7 times less mobile).[35,44] It should be noted that the stratigraphy of a fresco painting includes two mortars with different porosities. When applying a desalination protocol from the surface, the interface between the less porous external *intonaco* and the more porous inner *arriccio* could act as a barrier for the extraction of sulfates by the absorbent materials.

On the contrary, a removal of sulfate three times more efficient was achieved in the stratigraphy within the first 5 min when poultices were used. This can be explained by the lower water retention capacity of poultices against foams. The introduction of water in the system could promote a higher dissolution and diffusion of the sulfates to the absorbent material. Although poultices can extract more sulfates in the initial minutes of application, when increasing the application time, the extraction efficiency is lower compared with the foam (see Figure 1b). In addition, after 30 min, fluctuations of around $10.0 \pm 0.4\%$ in the extraction capacity of the poultices were observed. When applying the poultices for 24 h, a lower extraction percentage ($19.3 \pm 0.6\%$) was registered. This observation could suggest that at longer application periods, salt accumulations in inner regions of the wall painting could take place, as well as salt mobilizations from untreated internal areas of the central volume of the painting.

Although the capabilities of poultices can potentially be enhanced through successive application cycles and adjustments in grain packing, size, and formulation mixtures,[14] the data seem to indicate that our foams exhibit superior removal capacities.

2.2. Understanding the Extraction and Potential Redistribution of Salts after Desalination through Elemental Imaging

Quantitative distribution maps of the elements representing the salts were compared during the desalination experiment at different application times using both poultices and foams. As observed in **Figure 2**, the method of chloride impregnation in the mock-ups offered a quite homogeneous distribution of the salts in the stratigraphy, reaching an average distribution of $18.5 \pm 0.5\%$ and some accumulations up to $25.1 \pm 0.3\%$ in the lower and lateral parts of the mock-ups. This is probably due to a faster evaporation rate during drying in the mentioned areas.

Chlorine distribution maps in Figure 2 represent the progressive reduction of its concentration in the painting stratigraphy while increasing the application time of foams. In the first 5 min, the concentration of chlorine in the mock-ups decrease of an average of 5 orders of magnitude, considering all the areas in the stratigraphy. After 1 h (see Figure 2a), the central areas of the stratigraphy are completely free of chlorine (below the detection limit of μ-EDXRF) and some accumulations (100–200 μm in size) were detected on the edges of the section representing concentrations of chlorine of around $5.4 \pm 0.8\%$ and $7.0 \pm 0.3\%$. No further changes in distribution occurred after 8 h of application of the foams, being chlorine distributed in the section at concentrations lower than 0.06%.

In contrast, as observed in Figure 2b, poultices promote an irregular extraction of chlorides in the stratigraphy. Although the complete surface of the mock-ups was properly covered by the poultice, chloride extraction is restricted to a specific area and poultices are not able to extract chlorides located inner in the stratigraphy (see Figure 2b). Between 30 and 60 min of application, chlorides can be mobilized from inner to external parts in the stratigraphy, resulting in a salt front formation with a concentration close to the original salt loaded (*Class 3*). After 8 h, chlorides accumulated externally are extracted by the poultice, with no observable changes until 24 h of application. At this stage, poultices are not acting beyond 1 cm.

As in the case of chlorides, sulfates show a quite homogeneous in-depth distribution in the mock-ups (**Figure 3**). An average concentration of $12.3 \pm 1.1\%$ of sulfur, with accumulations reaching up to $17.3 \pm 0.6\%$ in the middle part and even $19.6 \pm 0.3\%$–$23.5 \pm 0.4\%$ in the rear lower sections were detected.

As observed in Figure 3, the migration of sulfates through the absorbent materials is lower than in the case of chlorides. Moreover, using poultices, the extraction of sulfates is reduced, and it takes place in restricted areas of the section (see Figure 3b). In the case of foams, multiple applications allow to promote the in-depth extraction of salts, being more difficult to extracts salts from inner areas of the stratigraphy. Between 0 and 30 min of application (see Figure 3a), the central region of the section showed accumulation of sulfates, probably attributed to mobilization. However, the gradient force and capillary action proved insufficient to allow a rapid migration of sulfates to the *intonaco*. It is noteworthy that no salt crystallizations were observed in the central areas enriched with sulfates. This may be attributed to the presence of an adequate wetting

Research Article
doi.org/10.1002/cmtd.202500052
Chemistry Europe
European Chemical Societies Publishing

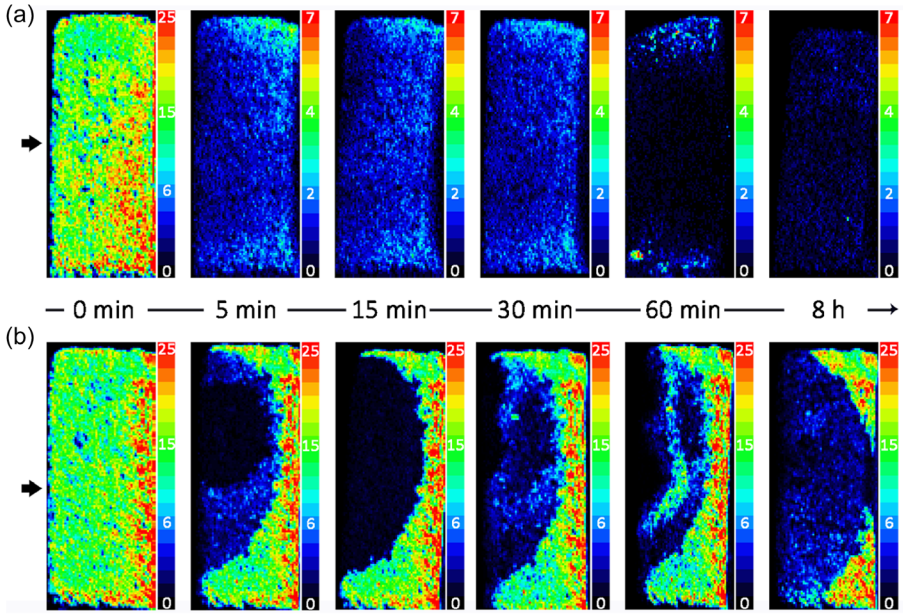

Figure 2. Monitoring of chloride removal in the section of the fresco painting mock-ups through quantitative distribution maps during desalination experiments using a) foams applied for 5, 15, 30, 60 min, and 8 h. A change of concentration scale between the maps at 0 and 5 min is necessary to show the remaining concentration of chlorine; b) poultices applied for 5, 15, 30, 60 min, and 8 h. The arrow indicates the application side. The numerical scales in the maps represent concentrations in wt%.

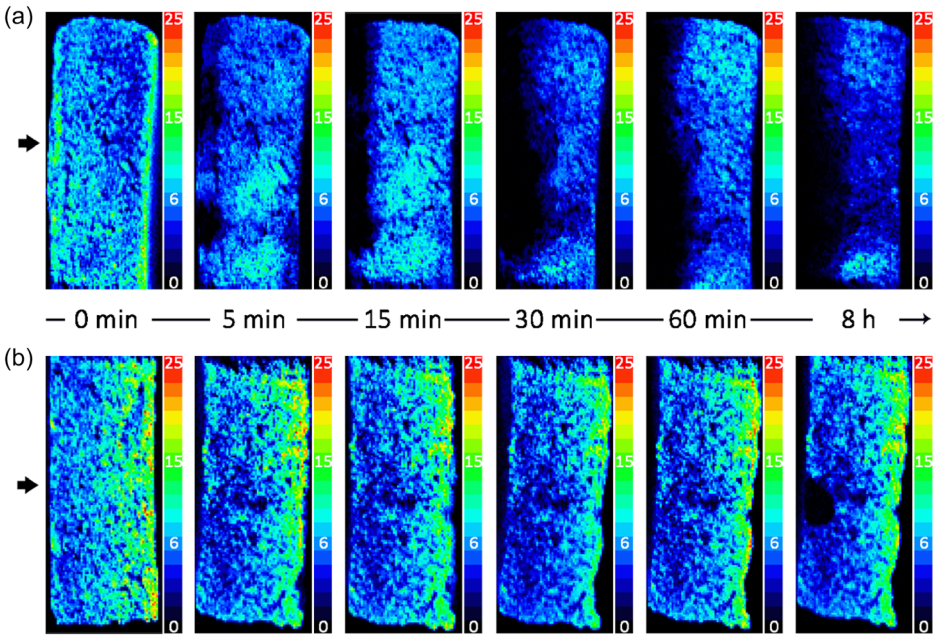

Figure 3. Monitoring of sulfates removal in the section of the fresco painting mock-ups through quantitative distribution maps during desalination experiments using a) foams applied for 5, 15, 30, 60 min, and 8 h; b) poultices applied for 5, 15, 30, 60 min, and 8 h. The arrow indicates the application side. Numerical scales in the maps represent concentrations in wt%.

phase on the substrate, which effectively prevented saturation. At longer times of application, sulfate redistribution and concentration were not visible, obtaining a reduction of more than one half of sulfur concentration even in the *arriccio* mortar. The remanent content of sulfur after longer application period is lower than 5.0%. Thus, foams proved to be able to reduce the original sulfate concentration to 0.1% in the stratigraphy of the painting, corresponding to a *Class 2* risk level with only one application.

2.3. Evaluation of the Potential Reusability of the Foams

To test the potential reusability of the micro-cellulose foams, mock-ups were impregnated with a mixture of chlorides and sulfates

Research Article
doi.org/10.1002/cmtd.202500052
Chemistry Europe
European Chemical Societies Publishing

(2 replicates). Foams were applied by sequential cycles of desalination of 15 min. After each application, foams were washed with 100 mL of Milli-Q water (by immersion) and manually squeezed, three times, before their reapplication. Foams not previously used in the desalination experiment were used for control purposes. Prior to reuse, potential salts present in the used foams were solubilized in water and quantified by ion chromatography after squeezing. Chlorides and sulfates were either undetectable or exhibited concentrations that were close to the detection limit.

To assess the potential damage in the micro-structure of the foam (with the associated loss of properties) derived from a continuous reuse, SEM micrographs (**Figure 4**) were obtained before and after several uses.

According to the microscopic observations, no significant alterations, such as fissures or fractures, were detected during the inspection of the foam section, and only a slight structural shrinkage could be perceived.

Sequential desalination cycles were continuously monitored using μ-EDXRF quantitative imaging from the surface to the cross section of each sample (see **Figure 5**). Scanning superficially the mock-ups before and after 15 min of application, a reduction of 87.2 ± 0.1% for chlorine and 74.0 ± 0.2% for sulfur was registered. Through two consecutive 15-min applications, a nearly complete reduction (96.8 ± 0.1%) of both salts was achieved, obtaining values close to the detection limit in the second application. After three cycles of application, salt content was reduced to around 0.03% in the mock-up section.

Focusing on the distribution of the characteristic elements associated to the impregnated salts, the chlorides are homogeneously distributed in the top part of the stratigraphy, with concentrations ranging from 9.4 ± 0.4 to 11.2 ± 0.3% of chlorine. (Figure 5a). In the inner areas of the *arriccio*, the concentration decreases to around 4.2 ± 0.4%. In the *arriccio*, a sulfate front of 14.4 ± 0.8% is observable, which decreases to concentrations

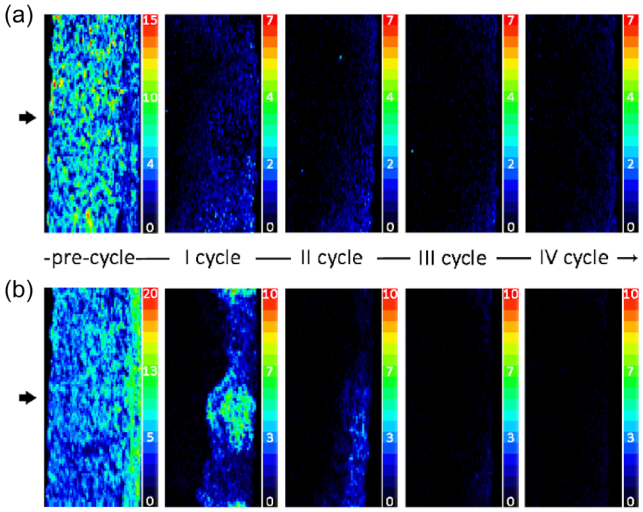

Figure 5. Quantitative distribution maps of a) chlorine and b) sulfur, before and after four cycles of desalination (15 min per application) by using micro-structured cellulose foam. The arrow indicates the application side. Numerical scales in the maps represent concentrations in wt%.

ranging from 7.1 ± 0.9% to 9.4 ± 1.1% in the outer areas of the painting stratigraphy (see Figure 5b). During desalination, after the first 15 min of application, the external areas of the stratigraphy were completely free of chlorine (or, better, this was below the limit of detection of the method), whereas the lower parts of the *arriccio* presented a uniform distribution of chlorine concentrations below 2.5 ± 0.2% (Figure 5a). After three applications of the foam all the chlorides were extracted beyond the limit of detection.

Regarding sulfates, the first application saw the removal of up to the first half of the *arriccio*. In the inner half of the *arriccio,* concentrations of sulfur of 3.5 ± 0.4% were detected (see Figure 5b). In the centre of the *arriccio*, an accumulation representing concentrations of sulfur of 6.4 ± 0.6% was observed. After the first

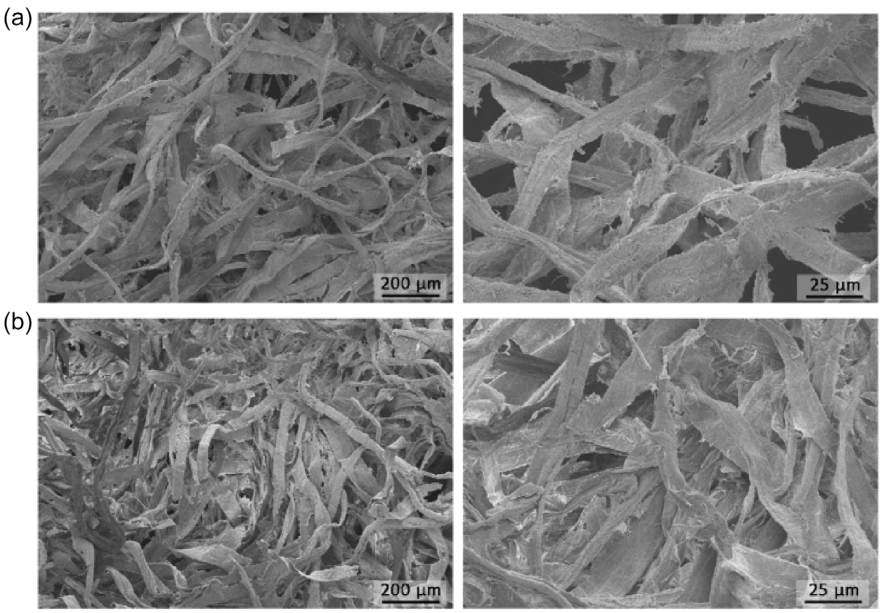

Figure 4. SEM micrographs showing the cross section of the micro-structured cellulose foams before a) and after b) being reused.

reuse of the foam, sulfates were successfully eliminated, not detecting changes in the sulfur concentration between the last two desalination cycles.

In addition, the back surface of the arriccio was also analyzed before and after cyclic desalination. Neither sulfur nor chlorine could be detected (see quantitative distribution maps in Figure S4 of the Supporting Information).

Considering that the pigment integrity could result affected by foam subsequent applications, the painting layer was monitored during the process through microscopic observations and colorimetric measurements. No evidence of morphological or colorimetric alterations were observed. Moreover, no residues from the foam were detected. In addition, no changes were registered in the quantitative distribution maps of iron before and after desalination (see Figure S5).

3. Conclusion

The comparative study of quantitative elemental distribution maps obtained by μ-EDXRF before and after desalination actions has proven to be a powerful methodology for assessing salt reduction at a microscopic scale, offering a more comprehensive understanding of the desalination mechanism in wall paintings. Although less sensitive than techniques like ion chromatography, we have demonstrated that μ-EDXRF can provide information about the elemental spatial distribution of salts during desalination while preserving the integrity of samples. The stratigraphic studies here presented showed that superficial monitoring is not enough to properly evaluate desalination protocols.

Specifically, this analytical approach allowed to compare the efficacy of a new alternative based on micro-structured cellulose foams, which offer significantly enhanced performance over conventional cellulose poultices for desalination of fresco paintings. Particularly, foams exhibit capacities that are 6 to 10 times higher when desalinating fresco paintings. Their highly porous microstructure provides higher water retention capacities, enhancing salt transport through the foam-painting system. These characteristics were crucial in achieving sulfate mobilization from deeper areas of the *arriccio* without creating salt accumulations in the painting stratigraphy during the migration process.

In contrast to conventional cellulose poultices, which require additional desalination cycles to achieve moderate efficacy, foams demonstrate superior performance in removing crystallized salts from inner stratigraphic areas, delivering optimal results in a significantly shorter timeframe. In future studies, it would be advisable to evaluate the versatility of these new materials for desalinating wall paintings with varying levels of damage caused by different crystallized salts and a wider palette of pigments.

The reusability potential of the foams has also been demonstrated. The incorporation of cellulose foams for conservation practices can mitigate waste generation and environmental footprint. With these materials, we pave the way to a gradual reduction of the consumption of raw materials over time, thereby decreasing the demand of cellulose production and its associated environmental impact.

4. Experimental Section

Reagents and Materials

CL-90 natural aerial lime paste (COM-CAL, classified according to UNE-EN 459 1:2015), fine sand of siliceous rock-based composition with a grain size of 2 mm (Sorigué S.A.U., Lleida, Spain) and white Carrara marble powder of a granulometry ranging from 0.7 to 1.2 mm (C.T.S. España S.L., Madrid) were used for *arriccio* and *intonaco* layer preparation in the fresco mock-up paintings. Hematite intense pigment (ref. #48651, Kremer Pigmente GmbH & Co. KG, Aichstetten, Germany) was used for the paint layer. Sodium chloride (99%, NaCl), and anhydrous sodium sulfate (99%, Na_2SO_4) were employed as salts to be impregnated in the mock-ups, and 10% solution of phenolphthalein (Merck KGaA, Darmstadt, Germany) to assess the carbonation process on fresco paintings mock-ups. Arbocel BC1000 was used to prepare cellulose poultices and Japanese paper 12.3 g when applying the poultices. Both were retrieved from C.T.S. España S.L.

Fresco Painting Mock-Ups: Preparation and Salt Impregnation

To study the efficiency of the proposed desalination strategies, fresco painting mock-ups reproducing the traditional Roman technique were prepared (Figure S1). Custom-made molds ($4 \times 4 \times 1.5$ cm^3) were employed to prepare the traditional three-layer stratigraphy, *arriccio*, *intonaco* and painting layer. Specifically, an *arriccio* made with sand and aerial lime paste (3:1), an *intonaco* of Carrara marble and aerial lime paste (2:1), and a last paint layer of hematite/water onto the wet mock-ups surface was used. To accelerate the carbonation, mock-ups were introduced in a Kesternich chamber for 21 days under saturated humidity with CO_2 at 40.2°C. The carbonation profile within the mock-up was assessed using the phenolphthalein test.[45]

NaCl and Na_2SO_4 solutions at 2.5% (w/v) were considered to infiltrate salts. These two salts were selected for this study because they are among the most commonly detected salts in wall paintings and are known to significantly contribute to their degradation.[46] Moreover, their differing physicochemical properties, such as solubility and response to environmental conditions, affect their behavior and impact on the substrate. Sodium chloride, typically associated with marine environments, is highly soluble and tends to migrate toward the upper sections of walls where it accumulates.[47] Its repeated cycles of dissolution and recrystallization driven by fluctuations of relative humidity lead to mechanical stress that damages the surface. In contrast, sodium sulfate exhibits lower solubility and mobility, typically precipitating in the lower areas of walls. Thenardite and mirabilite (among the—at least—eight different crystalline phases of sodium sulfate) have different solubilities. When thenardite (anhydrous form) dissolves during impregnation, it creates a highly supersaturated solution with respect to mirabilite (decahydrate). Such highly supersaturated solution in presence of mirabilite crystals is what exerts crystallization pressure and ultimately causes damage.[48–50]

To produce reproducible mock-ups in terms of homogeneity in the salt distribution, the mock-ups were vacuum-impregnated with salt solutions.[7,50] The removal of the air from the porous network allowed to infiltrate ions homogeneously. For this purpose, an adapted vacuum impregnation system[50] comprising of a desiccator connected to two parallel tubes to facilitate controlled access to the vacuum pump and the salt solution, was used (Figure S2). The mock-ups were then placed in the desiccator chamber, and vacuum was created and maintained. Afterwards, the salt solution was introduced until the entire mock-ups were submerged. Subsequently, the entry of air was carefully allowed to obtain a complete and homogenous distribution of the solution into the accessible porous network. After one hour, the mock-ups were recovered and dried at 105 °C for 24 h. Four replicates of chloride samples and sulfates were prepared. In

addition, a mixture solution of both salts at 3% (w/v) (1:1) was also used to impregnate the mock-ups.

The content (% weight) of independent salts infiltrated in the mock-ups was 0.25 ± 0.10% (gravimetrically determined). When infiltrating the mixture of salts, the content of salts in the mock-ups was 0.6 ± 0.18%. In both cases, the impact can be classified as Class 3 (high *salinity)* considering the Eureka EU 1270 rating.[51–53] This guideline defines risks and degradation degree by salts action according to five grades, that is; *Class 0*—very low (no harm of masonry), *Class 1*—low (constructions loaded with permanent source of capillary moisture can be damaged), *Class 2*—medium (the lifetime of plasters and paintings is shortened to a minimum), *Class 3*—high (the lifetime of plasters and paintings is significantly shortened), *Class 4*—extremely high (the construction will be severely damaged in a very short time).

Foams and Poultices Preparation

Briefly, to prepare cellulose poultices, Arbocel BC1000 powder was gradually added to distilled water (5 wt%) while stirring to avoid clumping. The mixture was settled for 30 min to fully hydrate and thicken. The poultice was spread over a Japanese paper in contact with the fresco mock-ups and maintained in contact for different periods of time. Japanese paper allowed to remove the poultice avoiding damaging the painted surface.

Cellulose foams with a uniform three-dimensional crosslinked microstructure were prepared under a patent-protected technology.[29] Briefly, commercial bleached softwood kraft pulp (hereinafter, cellulose fibers) were first oxidized. Freezing of this suspension leads to the formation of a 3D structure composed of interconnected fibers linked through cyclic acetal bonds, which, once thawed, behaves as a lightweight foam when it is dried or as a sponge when soaked in water. The foams were cut into pieces of 4 cm × 4 cm × 1.5 cm (weighing ca. 0.5 g), to cover the entire mock-up surface. Although the foam has a maximum water uptake capacity of 2000%, to make a comparative study, a similar water proportion used in the poultice preparation was loaded on the foam. After Milli-Q water addition, the possible water retained on the surface of the foam was removed. Due to its organized and stable structure, once wet, cellulose foam is stable enough to leave no residue on the paint surface. However, considering that traditionally with cellulose poultices Japanese paper is used between the poultices and the painting, to make a direct comparison, Japanese paper was also used between the foam to be applied and the surface of the painting (Figure S3).

Instruments

A Kesternich chamber (Spanish Society for Quality Control and Instrumentation, CCI) equipped with a high precision control module with a modifiable temperature range (20–50 °C) was used to accelerate the carbonation of the mock-ups. 2 L of CO_2 were introduced in the chamber to generate the acid atmosphere.

A dual M4 TORNADO μ-EDXRF spectrometer (Bruker Nano GmbH, Berlin, Germany) was used to quantitatively monitor the homogeneity in the distribution of the infiltrated salts and their reduction in the mock-ups after desalination experiments. The equipment has two micro-focus side window Rh X-ray tubes powered by low-power HV generators and cooled by air. In this case, one of the tubes able to work at 10–50 kV and 100–600 μA was used. This tube is connected to a poly-capillary lens that allows to work under a lateral/spatial resolution of 25 μm measured for Mo K_α (around 17 μm at 2.3 keV to 32 μm at 18.3 keV). The detection of the fluorescence radiation was performed using an XFlash silicon drift detector with a 30 mm^2 sensitive area and an energy resolution of 145 eV for Mn-K_α.

Elemental distribution maps were generated by extracting the K_α lines of the elements of interest from the acquired spectra. A careful balance between spectral resolution, spatial resolution, and acquisition time was achieved to obtain reliable analytical results within a reasonable measurement duration. Specifically, measurements were conducted with an acquisition time of 5 ms per pixel and a step size of 100 μm. To improve the detection sensitivity of lighter elements, all measurements were performed under vacuum conditions (20 mbar), given by a MV 10 N VARIO-B diaphragm pump (Vacuubrand, Wertheim, Germany), reducing air absorption and scattering. The resulting hyperspectral maps consist of 40,000 pixels, where each pixel contains a full X-ray fluorescence spectrum. This creates a multi-dimensional dataset, where two dimensions (*x* and *y*) correspond to the spatial coordinates of the scanned area, and a third dimension contains the fluorescence spectra at each point, represented by fluorescence intensity values across 4096 energy channels.

After assigning the elements present in each scanned mock-up, the sum spectrum of each scanning was recorded. To generate the quantitative maps of each element (Cl and S), the M-Quant software package (Bruker Nano GmbH, Germany) was used. Due to the changes of porosity during desalination, monitoring of salts reduction through the simple detection of counts was avoided. Instead, quantitative distribution maps were generated from the XRF hypercubes, considering the Kα lines of chlorine and sulfur and by applying the fundamental parameters (FP) method. The FP algorithm iteratively solves the Sherman equation, modeling the physics of X-ray interactions with the sample, including absorption, matrix effect, and sample geometry.[54]

In this work, the obtained quantitative distribution images are presented as maps of weight percentage. The calculation of the final quantitative distribution maps was performed every 2 pixels.

A Hitachi S4800 high-resolution SEM (Hitachi, Krefeld, Germany) was also employed to investigate the morphology of the micro-cellulose foams before and after its reuse. Before acquiring the micrographs, a conductive gold layer with a thickness of 15 nm was deposited on the foams using a Emitech K550X sputter coater system (Quorum Technologies, Lewes, UK). Images were acquired under a voltage of 5.0 kV.

Acknowledgements

This work has been supported by the project TED2021-129299A-I00, funded by MICIU/AEI/10.13039/501100011033 and by the European Union NextGenerationEU/PRTR. The authors gratefully acknowledge Open Access funding provided by University of Basque Country. M. Romani and O. Gomez-Laserna gratefully acknowledge their predoctoral and research fellowships, respectively, from ENCLOSURE project (TED2021-129299A-I00). A. Pitarch Martí is thankful for the contributions of the Serra Húnter Program. F. Caruso acknowledges his Maria Zambrano fellowship from UPV/EHU, funded by the Spanish Ministry of Universities and the European Union NextGenerationEU/PRTR. The authors are also grateful to the technical support provided by the Analytical and High-Resolution Microscopy laboratory of the SGIker (UPV/EHU).

Conflicts of Interest

The authors declare no conflicts of interest.

Data Availability Statement

The data that support the findings of this study are available from the corresponding author upon reasonable request.

Keywords: μ-EDXRF quantitative imaging · biopolymers · microstructured cellulose foams · Roman fresco wall paintings · salt removal

[1] E. Doehne, C. A. Price, *Stone Conservation: An Overview of Current Research*, 2nd ed., Getty Conservation Institute, Los Angeles **2010**.
[2] F. Mancinelli, in Proceedings of a Symposium Organized by the Courtauld Institute of Art and the Getty Conservation Institute, S. Cather ed., 13–16 July 1987, London, England, Getty Conservation Institute **1991**, pp. 57–66.
[3] F. Preusser, in Proc. of a Symposium Organized by the Courtauld Institute of Art and the Getty Conservation Institute, S. Cather ed., 13–16 July 1987, London, England, Getty Conservation Institute **1991**, pp. 1–12.
[4] R. A. J. Wüst, C. Schlüchter, *J. Archaeol. Sci.* **2000**, *27*, 1161.
[5] C. A. Price, *Archaeol. Int.* **2012**, *1*, 47.
[6] C. Rodriguez-Navarro, E. Doehne, *Earth Surf. Process. Landforms* **1999**, *24*, 191.
[7] F. Caruso, T. Wangler, R. J. Flatt, *J. Chem. Educ.* **2018**, *95*, 1615.
[8] A. E. Charola, *J. Am. Inst. Conserv.* **2000**, *39*, 327.
[9] M. Cotte, J. Susini, N. Metrich, A. Moscato, C. Gratziu, A. Bertagnini, M. Pagano, *Anal. Chem.* **2006**, *78*, 7484.
[10] S. Pérez-Diez, A. P. Martí, A. Giakoumaki, N. Prieto-Taboada, S. F.-O. de Vallejuelo, A. Martellone, B. De Nigris, M. Osanna, J. M. Madariaga, M. Maguregui, *Anal. Chem.* **2021**, *93*, 15870.
[11] J. M. P. Q. Delgado, A. S. Guimarães, V. P. de Freitas, I. Antepara, V. Kočí, R. Černý, *Adv. Mater. Sci. Eng.* **2016**, *2016*, e1280894.
[12] M. Steiger, A. E. Charola, K. Sterflinger, S. Siegesmund, R. Snethlage, in *Stone in Architecture: Properties, Durability* (Eds: S. Siegesmund, R. Snethlage), Springer, Berlin, **2014**, pp. 225–316.
[13] E. Doehne, in Proc. of the 11th Int Congress on Deterioration and Conservation of Stone, 15–20 September 2008, Torun, Poland **2008**, pp. 1–8.
[14] V. Vergès-Belmin, A. Heritage, A. Bourgès, *Stud. Conserv.* **2011**, *56*, 281.
[15] M. B, F. Bandini, A. Felici, M. R. Lanfranchi, R. Negrotti, C. Riminesi, D. Scalarone, A. Sansonetti, *IOP Conf. Ser.: Mater. Sci. Eng.* **2018**, *364*, 012076.
[16] I. Egartner, O. Sass, *Herit. Sci.* **2016**, *4*, 41.
[17] A. Sawdy, B. Lubelli, V. Voronina, L. Pel, *Stud. Conserv.* **2010**, *55*, 26.
[18] V. Vergès-Belmin, H. Siedel, *Restor. Build. Monum.* **2005**, *11*, 391.
[19] E. Ferroni, V. Malaguzzi-Valerj, G. Rovida, in Proc. of the ICOM Conf., Amsterdam, Holland **1969**, pp. 1–12.
[20] D. Chelazzi, P. Baglioni, *Langmuir* **2023**, *39*, 10744.
[21] D. Chelazzi, G. Poggi, Y. Jaidar, N. Toccafondi, R. Giorgi, P. Baglioni, *J. Colloid Interface Sci.* **2013**, *392*, 42.
[22] Y. Ye, L. Yu, E. Lizundia, Y. Zhu, C. Chen, F. Jiang, *Chem. Rev.* **2023**, *123*, 9204.
[23] A. Etale, A. J. Onyianta, S. R. Turner, S. J. Eichhorn, *Chem. Rev.* **2023**, *123*, 2016.
[24] T. Li, C. Chen, A. H. Brozena, J. Y. Zhu, L. Xu, C. Driemeier, J. Dai, O. J. Rojas, A. Isogai, L. Wågberg, L. Hu, *Nature* **2021**, *590*, 47.
[25] K. J. De France, T. Hoare, E. D. Cranston, *Chem. Mater.* **2017**, *29*, 4609.
[26] C. Antonini, T. Wu, T. Zimmermann, A. Kherbeche, M.-J. Thoraval, G. Nyström, T. Geiger, *Nanomaterials* **2019**, *9*, 1142.
[27] B. Aoudi, Y. Boluk, M. G. El-Din, *Sci. Total Environ.* **2022**, *843*, 156903.
[28] N. Lavoine, L. Bergström, *J. Mater. Chem.* **2017**, *5*, 16105.
[29] Á. T. Etayo, A. S. Polo, J. H. Betanzos, M. A. Lakuntza, I. Svensson (World Intellectual Property Organization (WIPO)), WO 2016079140 A1, **2016**.
[30] S. Ma, C. Liu, Y. Xu, L. Wang, H. Wang, W. Xu, Y. Zhuang, H. Yang, *J. Phys. Chem. B.* **2021**, *125*, 5853.
[31] B. D. Dinneen, J. B. Abel, R. Stein, *J. Am. Inst. Conserv.* **2024**, *63*, 309.
[32] A. Sansonetti, C. Riminesi, S. Mironiouk, N. Proietti, V. Di Tullio, R. Nisticò, B. Sacchi, C. Canevali, *Gels* **2024**, *10*, 708.
[33] R. Snethlage, S. Siegesmund, R. Snethlage, in *Stone in Architecture: Properties, Durability* (Eds: S. Siegesmund, R. Snethlage), Springer, Berlin **2014**, p. 415.
[34] P. Bosch-Roig, H. Allegue, I. Bosch, *Sustainability* **2019**, *11*, 4227.
[35] O. Gómez-Laserna, N. Prieto-Taboada, H. Morillas, I. Arrizabalaga, M.Á. Olazabal, G. Arana, J. M. Madariaga, *Anal. Methods* **2015**, *7*, 4608.
[36] O. Gómez-Laserna, I. Arrizabalaga, N. Prieto-Taboada, M.Á. Olazabal, G. Arana, J. M. Madariaga, *Anal. Bioanal. Chem.* **2015**, *407*, 5635.
[37] P. Irizar, O. Gomez-Laserna, G. Arana, J. M. Madariaga, I. Martínez-Arkarazo, *J. Cult. Herit.* **2023**, *64*, 12.
[38] M. Romani, L. Pronti, C. Ruberto, L. Severini, C. Mazzuca, G. Viviani, A. Mazzinghi, M. Chiari, L. Castelli, F. Taccetti, A. Damiani, C. Gorga, M. Angelucci, M. Cestelli-Guidi, *Eur. Phys. J. Plus* **2022**, *137*, 757.
[39] S. Manohar, M. Santhanam, *Curr. Sci.* **2021**, *121*, 1307.
[40] A. Bourgès, V. Vergès-Belmin, *Mater. Struct.* **2011**, *44*, 1233.
[41] V. Vergès-Belmin, A. Bourgès, in Proc. of the Int. Congress on Salt Weathering on Buildings and Stone Sculptures, 22–24 October 2008, Copenhagen, Denmark **2008**, pp. 29–41.
[42] C. Canevali, M. Lanfranchi, H. Tanday, C. Corti, D. Monticelli, L. Rampazzi, M. Bertasa, A. Sansonetti, *J. Cult. Herit.* **2021**, *51*, 166.
[43] L. Pel, A. Sawdy, V. Voronina, *J. Cult. Herit.* **2010**, *11*, 59.
[44] R. Chang, J. Overby, *Chemistry*, 14th ed., McGraw-Hill Education, New York **2010**.
[45] D. O. McPolin, P. A. Basheer, A. E. Long, *J. Mater. Civ. Eng.* **2009**, *21*, 217.
[46] S. Pérez-Diez, L. J. Fernández-Menéndez, H. Morillas, A. Martellone, B. De Nigris, M. Osanna, N. Bordel, F. Caruso, J. M. Madariaga, M. Maguregui, *Angew. Chem., Int. Edit.* **2021**, *60*, 3028.
[47] A. Arnold, K. Zehnder, in *The Conservation of Wall Paintings* (Ed: S. Cather), Getty Conservation Institute, Los Angeles **1991**, p. 103.
[48] N. Tsui, R. J. Flatt, G. W. Scherer, *J. Cult. Herit.* **2003**, *4*, 109.
[49] R. J. Flatt, *J. Cryst. Growth* **2002**, *242*, 435.
[50] R. J. Flatt, F. Caruso, A. M. A. Sanchez, G. W. Scherer, *Nat. Commun.* **2014**, *5*, 4823.
[51] P. Šťastný, J. Gašparík, O. Makýš, *J. Build. Eng.* **2021**, *41*, 102785.
[52] M. Pavlíková, Z. Pavlík, M. Keppert, R. Černý, *Constr. Build. Mater.* **2011**, *25*, 1205.
[53] E. P. Guerra, *Risanamento di murature umide e degradate*, 5th ed., Dario Flaccovio Editore, Palermo **2020**.
[54] S. Flude, M. Haschke, M. Storey, *Mineral. Mag.* **2017**, *81*, 923.

Manuscript received: April 17, 2025
Revised manuscript received: June 8, 2025
Version of record online: